NASA TECHNICAL NOTE

NASA TN D-2614

NASA TN D-2614

FACILITY FORM 602

N65 15529 (ACCESSION NUMBER) (THRU)

18 (PAGES) 1 (CODE)

(NASA CR OR TMX OR AD NUMBER) 31 (CATEGORY)

GPO PRICE $ _____

OTS PRICE(S) $ 1.00

Hard copy (HC) _____

Microfiche (MF) .50

SOLAR SIMULATION TESTING OF AN EARTH SATELLITE AT GODDARD SPACE FLIGHT CENTER

by R. E. Bernier, R. H. Hoffman, A. R. Timmins, and E. I. Powers

Goddard Space Flight Center
Greenbelt, Md.

NATIONAL AERONAUTICS AND SPACE ADMINISTRATION • WASHINGTON, D. C. • JANUARY 1965

SOLAR SIMULATION TESTING OF AN EARTH SATELLITE

AT GODDARD SPACE FLIGHT CENTER

By R. E. Bernier, R. H. Hoffman,
A. R. Timmins, and E. I. Powers

Goddard Space Flight Center
Greenbelt, Md.

NATIONAL AERONAUTICS AND SPACE ADMINISTRATION

For sale by the Office of Technical Services, Department of Commerce,
Washington, D.C. 20230 -- Price $1.00

SOLAR SIMULATION TESTING OF AN EARTH SATELLITE AT GODDARD SPACE FLIGHT CENTER

by
R. E. Bernier, R. H. Hoffman
A. R. Timmins, and E. I. Powers
Goddard Space Flight Center

SUMMARY

15529

The results of a solar simulation test, as well as the testing techniques used, on the flight backup Ariel II (UK-2/S-52) international ionosphere satellite are presented. The satellite was subjected to carbon-arc solar simulation at 10^{-6} torr vacuum, with liquid-nitrogen shroud wall temperature. It was rotated at 3 rpm to simulate orbital spin and was tested at several attitudes relative to the incident solar energy.

The major objectives of the test were to operate the spacecraft under simulated dynamic space conditions and to evaluate the spacecraft thermal design. The results verified the design and demonstrated successful operation of the spacecraft over the entire range of design temperatures and dynamic temperature changes.

author

CONTENTS

Summary i

INTRODUCTION 1

OBJECTIVES OF THE TEST 1

THERMAL DESIGN AND PREDICTIONS 2

- Determination of the Thermal Model 2
- Conduction and Radiation Interchange 4
- Solar Input 4
- Albedo and Earthshine 4
- Modifications in the Thermal Analysis 4

DESCRIPTION OF THE SOLAR SIMULATION TEST 5

PROBLEMS ASSOCIATED WITH SOLAR SIMULATION 7

- Spectrum 7
- Uniformity and Degradation of the Carbon-Arc Solar Simulator 7
- Determination of Carbon-Arc Intensity 8
- Intensity Calibration and Monitoring of the Carbon-Arc Solar Simulator . . . 9
- Beam Collimation 10
- Determination of Local Solar Intensity Input to the Spacecraft 10

SOLAR SIMULATION TEST RESULTS 12

CONCLUSIONS 13

References 14

SOLAR SIMULATION TESTING OF AN EARTH SATELLITE AT GODDARD SPACE FLIGHT CENTER*

by
R. E. Bernier, R. H. Hoffman
A. R. Timmins, and E. I. Powers
Goddard Space Flight Center

INTRODUCTION

The use of solar simulation to evaluate the thermal performance of a spacecraft is still relatively new and controversial. Reference 1 reports successful use of carbon arcs in testing the Telstar spacecraft. Additional information on the use of the carbon arc as a solar source should be useful in evaluating its effectiveness as a thermal design technique. At Goddard Space Flight Center carbon arcs have been used for achieving the solar simulation testing of spacecraft sized for the Delta and Scout boosters. This report presents data and experience from such testing, using the results from the flight backup Ariel II (UK-2/S-52) international satellite† as an example.

OBJECTIVES OF THE TEST

The primary purpose of exposing a spacecraft to a simulated solar atmosphere is to verify the thermal design of the spacecraft in full operation.

An additional objective is to check the operation of experiments in the vacuum chamber with simulated solar energy. Some experiments are directly stimulated by the sun, as in the case of ozone measurement experiments on the UK-2/S-52. Others, such as the micrometeoroid detector, use sunlight as a secondary medium by measuring the amount of sunlight passing through the punctures in a foil. Spacecraft subsystems also use sunlight as an event marker, switching operational modes as a sunrise or sunset condition is encountered.

A benefit derived from a solar test of a spacecraft is the exposure of spacecraft coatings and exposed surfaces to the thermal radiation environment encountered in orbit. In this way, possible physical incompatibilities may be discovered.

*Presented by Mr. Bernier at the Institute of Environmental Sciences 1964 Technical Meeting and Equipment Exposition, Philadelphia, April 13-15. Published in *1964 Proceedings*, pp. 209-216.

†Ariel II was launched successfully March 27, 1964 (designation: 1964-15A). The initial orbital temperature data compared favorably with prelaunch predictions.

For these reasons, as well as the basic desire of environmental testing groups to demonstrate spacecraft performance under the simulated environment, a solar test of the UK-2/S-52 international satellite was conducted.

THERMAL DESIGN AND PREDICTIONS

As previously stated, the primary purpose of conducting a solar test is to verify the thermal design of the spacecraft. Therefore, a brief discussion of the radiation inputs and the thermal model is presented so that a better appreciation of the test results may be possible.

For the UK-2/S-52, internal power dissipation is relatively small, compared with the total radiation input, and does not have a significant effect on the satellite mean temperature. In general, the magnitude of this effect depends on the emittance ϵ and the surface area (e.g., with a surface of low absolute ϵ, internal power may raise the temperature significantly because the skin has a limited capacity for reradiation).

Direct solar heating, earth-reflected solar heating (albedo), and earth-emitted radiation (earthshine) represent the significant inputs to the satellite. It is apparent that an adequate thermal design is predicated on a reasonably accurate knowledge of these thermal radiation inputs. The major source of energy–direct solar radiation–is, fortunately, the most accurate obtained. Since the sun's rays impinging on the satellite are virtually parallel, the problem is simply one of determining the instantaneous orientation of each external face with respect to the solar vector.

Determination of the Thermal Model

Of prime importance in the thermal analysis of a spacecraft is the determination of the thermal model. The model, an approximate mathematical representation of the satellite, is composed of a number of isothermal nodes or areas. The selection of these nodes is governed partly by convenience in working around interfaces, by accuracy requirements, and by a desire to minimize engineering and computer time.

First inspection of the UK-2/S-52 (Figure 1) showed that the broadband ozone detector mounted on top of the spacecraft was essentially independent of the spacecraft itself. Therefore, separate thermal models were developed for the main spacecraft and the detector and were thermally coupled by radiation and conduction interchange. The spacecraft was divided into 20 nodes, and the broadband ozone detector into 19 nodes.

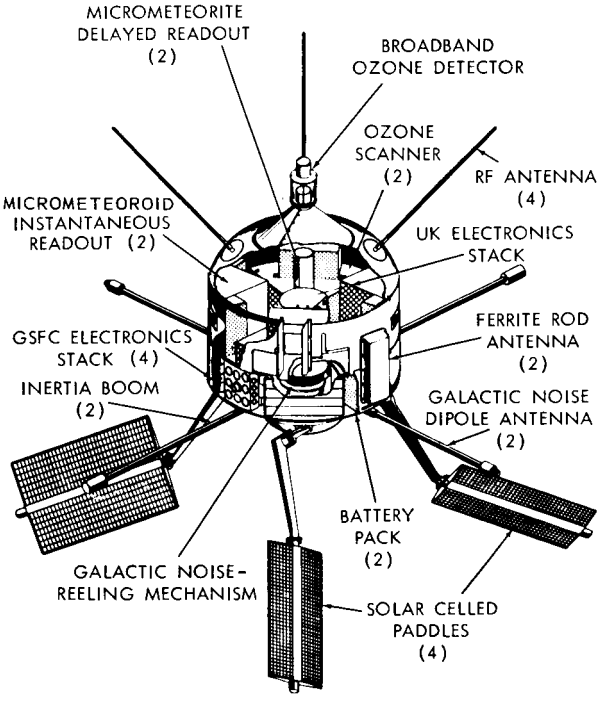

Figure 1–Flight backup Ariel II.

The thermal model of the ozone detector is shown in Figure 2. The most critical elements of this experiment are the monitor cell and the thorium-coated glass-enclosed tube at the top, each of which must be maintained below 60 °C.

The thermal model of the spacecraft is shown in Figure 3. Since the satellite is spinning about its longitudinal axis, skin temperatures tend to be uniform about the axis. This, together with the symmetrical design of the spacecraft, greatly simplifies the thermal considerations. As Figure 1 illustrates, there are a few components exposed to space: the ferrite rod antennas mounted in two fiber glass containers, the foil of the four micrometeoroid experiments, and the four apertures of the ozone scanners. There are also several openings in the bottom dome around the boom and paddle arm mounts which expose certain internal elements to space.

Since elements exposed to space generally undergo significant fluctuations in temperature, three of the ten external nodes were assigned to the ferrite rods, micrometeoroid foil, and the ozone scanner apertures. Of the ten internal nodes, five are structural elements and five relate to the experiments. The experiments on the upper shelf were considered as one node, since each is similarly influenced by the temperatures of of the upper dome and midskin while the power dissipated is negligible. The equipment on the lower shelf also was considered as one node.

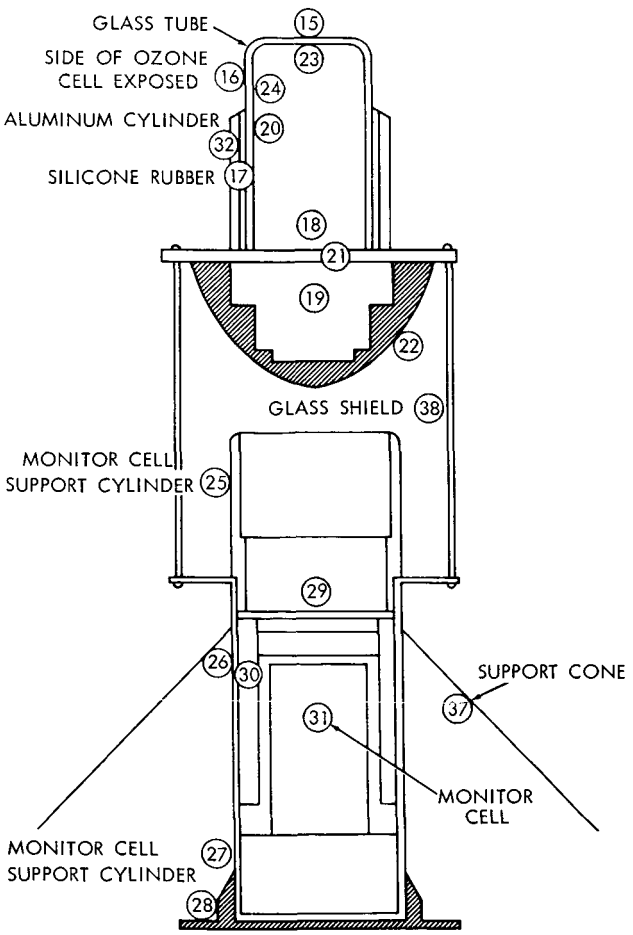

Figure 2–Broadband ozone detector node locations.

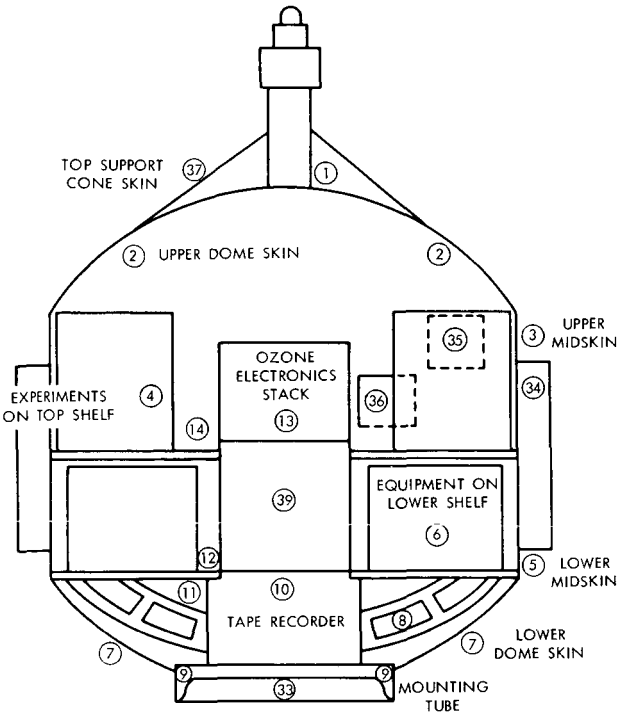

Figure 3–Thermal model for flight backup Ariel II, main body node locations.

The batteries, however, were investigated in further detail because of local hotspots while being charged. The three remaining internal nodes represent the ozone electronics stack, the galactic noise-reeling mechanism, and the tape recorder.

Conduction and Radiation Interchange

Every node is thermally coupled to one or more nodes by conduction and/or radiation interchange. External nodes also radiate to space. To determine the radiative coupling, the shape-factor area product and the effective emittance between nodes were determined. The shape-factor calculations were simplified by reducing the internal nodes to simple geometric forms (flat plates, cylinders, spheres, etc.) and by employing sources such as Reference 2. Almost the entire interior of the spacecraft was painted black to minimize thermal gradients. The effective emittance values were, therefore, approximately equal to 1.

The conduction interchange presented a problem in some cases since there was no way of accurately determining the conductance across joints. In these cases the extremes were considered, assuming both perfect contact and virtual isolation of the two nodes to determine how large a gradient might exist. Ten percent of perfect contact area was usually used for a nominal value.

Solar Input

As mentioned earlier, the major source of heat input to an orbiting satellite is direct solar radiation. The solar radiation absorbed by an external surface is $SA_p\alpha$, where S is the solar constant, A_p is the projected area to sunlight, and α is the solar absorptance of the surface.

Determining the projected areas of each surface element or node for different positions around the spin axis and for various aspect angles was accomplished by taking pictures of a one-fifth-scale model of the spacecraft. The satellite was designed to operate within solar aspect angles (angle between the solar vector and spin axis) of 45 to 135 degrees. However, for a complete analytical study the projected areas were determined for all aspect angles at 15-degree increments.

Albedo and Earthshine

A computer program (Reference 3) was employed to determine the values of albedo and earthshine incident upon the rotating surfaces throughout the orbit. Average orbital values were used for the two orbits considered. Albedo and earthshine account for approximately 15 to 30 percent of the total external heat input, albedo being greater in the minimum sunlight orbit.

Modifications in the Thermal Analysis

In altering the thermal analysis for use in the solar environment test chamber, the energy inputs of albedo and earthshine were equated to zero since no attempt was made in the test to simulate them. The effect of paddle shading at high aspect angles also was removed from the computer analysis since the test was conducted without the solar paddles fixed to the spacecraft.

Calibration tests were performed on samples of the spacecraft coatings to determine their absorptance properties when illuminated by the solar simulator in the test chamber. These properties were then inserted into the thermal model in place of the values used for orbital predictions. It is noted here that the difference between the orbital absorptance properties and the carbon-arc chamber values for the UK-2/S-52 coatings was negligible. However, the practice of using test-condition absorptance properties to predict test temperatures can be extremely important when a source with a poor spectral match is used on a coating whose absorptance response is not flat in the source wavelength region.

The thermal model was used to predict spacecraft temperatures from carbon-arc radiation intensity values which were introduced as input fluxes to the external nodes of the spacecraft. Agreement between predicted and actual test temperatures would then corroborate the thermal design of the spacecraft. Differences in predicted versus test temperatures would indicate areas requiring more study, either in the design or in the test technique.

DESCRIPTION OF THE SOLAR SIMULATION TEST

The test was performed in a 7-foot-diameter, 8-foot-long, cylindrical thermal-vacuum chamber. Located at one end of the chamber is a 1-foot-diameter quartz port through which the carbon-arc beam was introduced (Figure 4).

The spacecraft was mounted on a rotator-gimbal mount which provided two-axis motion: spin about the centerline of the spacecraft at 3 rpm, and inclination relative to the incident simulated solar radiation. Because of the physical limitations of the facility size, the inertia booms, galactic noise experiment dipole booms, and solar paddles were not included in the test configuration. Also, shortened telemetry antennas were substituted for the full-length antennas during this test (Figure 5). Two modes of information were available from the spacecraft: normal telemetry

MANUFACTURER
Goddard Space Flight Center (Prime)

TEMPERATURE (HEAT SINK)
-173 °C (100 °K)

SOLAR SIMULATION
1400 watts/m^2 over a 91 cm (3 ft) diam. circle by carbon arc

ULTIMATE VACUUM
5×10^{-8} mm Hg

TIMES TO PRESSURES
1×10^{-6} mm Hg — 3 hours
5×10^{-8} mm Hg — 15 hours

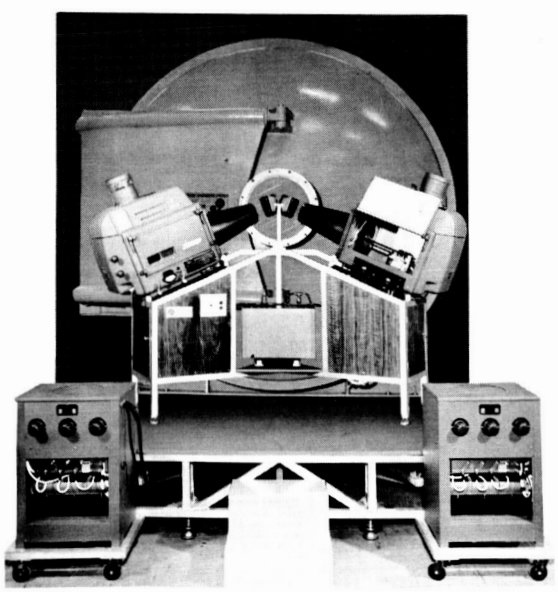

Figure 4—The environment simulator.

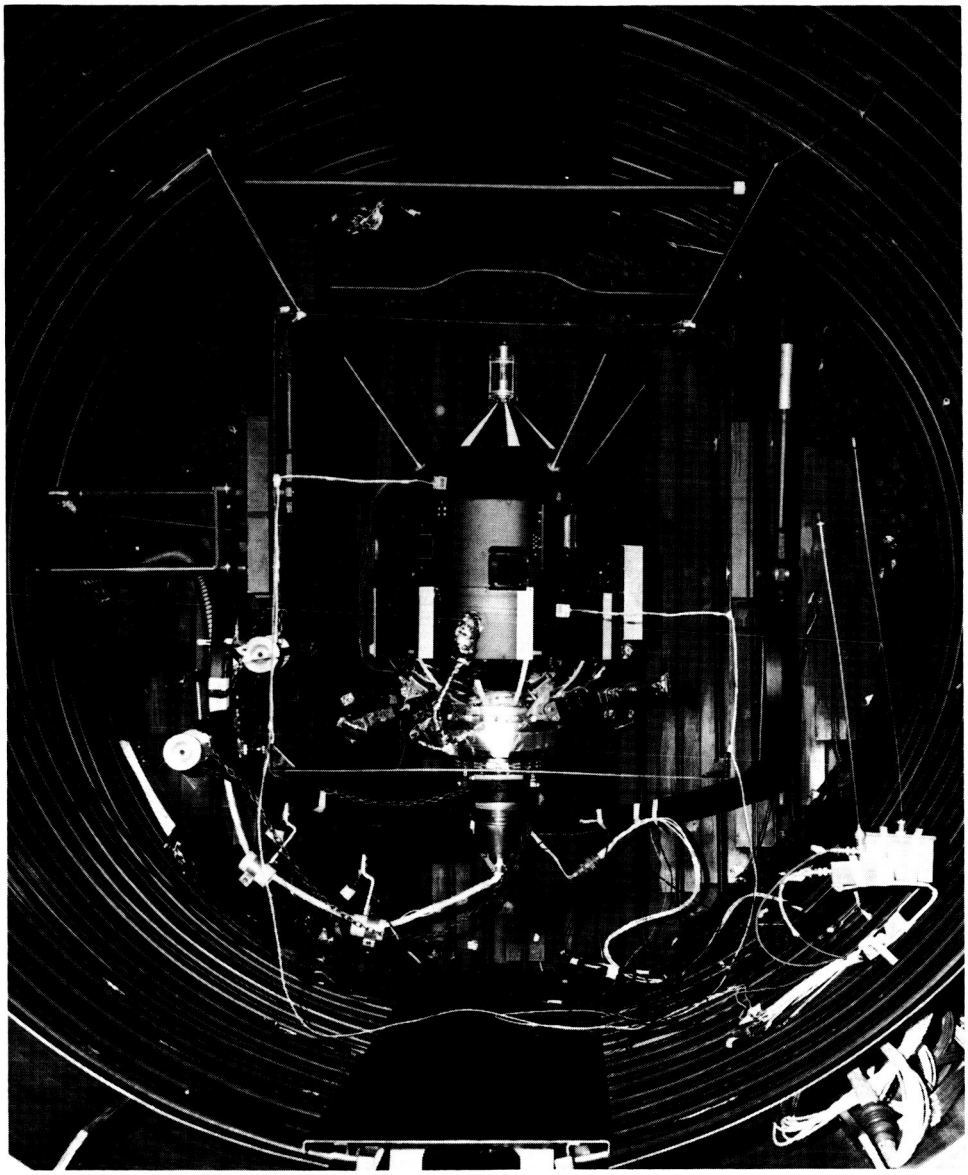

Figure 5—Flight backup Ariel II mounted on rotator-gimbal in the thermal-vacuum chamber.

transmission and command receiver, and a test hardline-slipring combination for power and supplementary data. The former system provided information in the same format as its orbital operation, while the latter provided the capability of recharging the on-board batteries and transmitting data from temperature sensors mounted for test purposes. These sensor outputs were scanned during the test to minimize the number of sliprings.

The pressure environment was in the range of 1×10^{-7} mm Hg, while the chamber walls were at approximately liquid-nitrogen temperature, -190 °C. The simulated solar radiation was set at an equivalent 1 solar constant, as described in the next section of this report. The spacecraft was fully operational from an experiment and subsystem basis while rotating on its spin axis.

The spacecraft was separated from the rotator-gimbal mount by a nylon insulator. Heat was supplied to the mount to such a degree that a small temperature gradient existed at all times. This minimized the energy flow between the spacecraft and mount. Since the temperatures were monitored throughout the test, approximate values of heat gain or loss were calculated. These values were introduced into the thermal model, to be reflected in the spacecraft energy balance and test temperature predictions.

Three spacecraft-incident solar radiation aspects were tested. They consisted of the 90-degree aspect or broadside solar exposure, the 45-degree aspect or maximum top-to-bottom temperature gradient expected in flight, and the 135-degree aspect or maximum bottom-to-top temperature gradient expected.

The variation of sun exposure in orbit is from 63 to 100 percent. The 63-percent exposure consisted of a series of cycles of 55-minute sunlight–32-minute shade periods. The 90-degree aspect position was tested at both of the above exposures to determine the effect on mean spacecraft temperature. The remaining aspects of 45 and 135 degrees were tested at the 100 percent sunlight condition only, because the primary objective was to study the internal temperature gradients resulting from these aspects.

PROBLEMS ASSOCIATED WITH SOLAR SIMULATION

Some of the difficulties encountered in attempting to simulate solar radiation are related below. The efforts to compensate for these problems are discussed in detail.

The choice of radiation source in large part is dictated by the desire to match as closely as possible the spectrum of the sun at orbital altitude. In addition, the ease of handling the source during the test must be considered.

Spectrum

Any significant departure in the spectral distribution of the simulator source from the sun's spectrum, as defined in the Johnson Curve, may cause a change in the absorbed energy of the exposed surface.

The carbon arc was chosen as the solar source because of its close spectral match with the Johnson Curve. Open-arc sources, however, present several operational problems, as discussed in the following paragraphs.

Uniformity and Degradation of the Carbon-Arc Solar Simulator

The carbon-arc system consisted of two modified reflector arc lamps. The system contained no optics except the quartz port in the vacuum chamber. Two arc lamps were used for two reasons: (1) the carbon-rod feed mechanism created a shadow on the reflector and a discontinuity in

the intensity of the beam from a single lamp; (2) the necessity for replacing the consumable rod in each lamp every hour warranted the use of multiple lamps to minimize the interruption of radiation energy input to the spacecraft.

The use of a reflector system is beneficial from a power and efficiency standpoint but creates uniformity and degradation problems. The exposure of the reflector to the open arc permits the deposit of vaporized carbon on the reflector surface, resulting in loss of reflectance efficiency and an ever-changing intensity distribution in the projected beam. To compensate for this condition during the test, intensity mappings of the projected beam were made at selected intervals in the test cycle. A rolled-ribbon thermocouple radiometer mounted on an X-Y plotting board was used for this mapping procedure. This provided an in-test calibration of the radiation beam and also a reference point for total intensity adjustment to compensate for reflector degradation.

Determination of Carbon-Arc Intensity

The first step in determining the arc intensity or solar flux on the spacecraft is to determine the effective α/ϵ of the total spacecraft when illuminated by the natural sun. This is combined with the carbon-arc intensity I_c and the natural sun intensity I_s as follows:

$$I_s \, (\alpha/\epsilon)_s = I_c \, (\alpha/\epsilon)_c \quad . \tag{1}$$

The effective α/ϵ is determined by the following equations:

$$\alpha_{eff} = \bar{A}_1 \, \alpha_1 + \bar{A}_2 \, \alpha_2 + \cdots \bar{A}_n \, \alpha_n \quad , \tag{2}$$

$$\epsilon_{eff} = \bar{A}_1 \, \epsilon_1 + \bar{A}_2 \, \epsilon_2 + \cdots \bar{A}_n \, \epsilon_n \quad , \tag{3}$$

$$(\alpha/\epsilon)_{eff} = \frac{\alpha_{eff}}{\epsilon_{eff}} \quad , \tag{4}$$

where

$\bar{A}$ = ratio of coating area to total exposed area (as given in Table 2),

α = absorptance,

ϵ = emittance.

Table 1

Spacecraft Coating Thermal Properties

Coating	Solar			Chamber		
	α	ϵ	α/ϵ	α	ϵ	α/ϵ
Black	0.96	0.86	1.12	0.96	0.86	1.12
White	0.27	0.86	0.31	0.26	0.86	0.30
Evap. aluminum	0.12	0.04	3.0	0.11	0.04	2.77

By referring to Tables 1 and 2, which give the coating thermal properties and their areas, respectively, the following effective α/ϵ ratios are derived:

$$(\alpha/\epsilon)_{eff,\ solar} = 1.04 \quad , \tag{5}$$

$$(\alpha/\epsilon)_{eff,\ chamber} = 1.03 \quad . \tag{6}$$

Table 2

Spacecraft Coating Area Evaluation

Spacecraft Surface	Area (sq ft)	Percent of Total Area	White (%)	White (% of total area)	Black (%)	Black (% of total area)	Evap. Al (%)	Evap. Al (% of total area)	Al Foil (%)	Al Foil (% of total area)
Top dome	2.82	23.7	0	0	100	23.7	0	0	0	0
B. B. support dome	1.16	9.8	25	2.5	75	7.5	0	0	0	0
Upper mid-skin	2.50	21.0	0	0	100	21.0	0	0	0	0
Lower mid-skin	2.58	21.7	20	4.3	80	17.4	0	0	0	0
Bottom dome	2.53	21.3	10	2.1	0	0	90	19.2	0	0
Mounting ring	0.30	2.5	0	0	0	0	0	0	100	2.5
Total area:	11.89			8.9		69.6		19.2		2.5

Combining Equations 1, 5, and 6, gives, assuming I_s = 1 solar constant,

$$I_c = 1.01 \text{ solar constant} \tag{7}$$

Intensity Calibration and Monitoring of the Carbon-Arc Solar Simulator

The lack of an absolute solar standard detector made it necessary to use a secondary method of intensity calibration. The method chosen was the integrating black-ball technique in which a thin-shell aluminum ball, the approximate size of the spacecraft, is placed in the test chamber in the exact location the spacecraft will occupy during the test. The integrating ball has a small thin-shell ball suspended in its center. The inner ball temperature is measured by a thermocouple. Both balls are coated with a black paint of known absorptance and emittance. A calculation is made to determine the stabilization temperature of the ball for a flux of 1.01 solar constant. The chamber is then evacuated, and the shrouds are flooded with liquid nitrogen to simulate the same environment that the spacecraft will encounter. The arc output is adjusted so that the ball system stabilizes to the predetermined temperature. Once this focus adjustment is made, the arc beam is mapped for uniformity and intensity with the radiation detector on the X-Y plotting board located external to the chamber. The readings of the detector are then bench-marked to the intensity incident on the black ball and are used throughout the test of the spacecraft as a relative monitoring point.

The use of the black-ball technique for calibrating the arcs serves a dual purpose: (1) arc calibration as described above, and (2) inclusion of inherent chamber energy (reflected or radiative) in the calibration of total energy absorbed by the black ball. The black coating of the ball is spectrally flat in its absorption characteristics, and therefore arrives at the desired stabilization temperature by summing the energies from the carbon arcs and the inherent chamber sources.

This technique is applicable if the spacecraft to be tested also is essentially spectrally flat in its absorption characteristics, as in the case of the UK-2/S-52.

Beam Collimation

The radiation beam projected by the solar simulator is divergent with a $7\frac{1}{2}$-degree half-angle. This permits the system to project a 36-inch-diameter beam at the centerline plane of the spacecraft. This divergence rate is not considered severe enough to cause unnatural shadowing; however, a measured energy change per unit area of approximately 1 percent per inch of depth variation is produced in the test volume. Therefore, incident intensity compensation was made to the thermal model of the spacecraft to take into account this change of intensity with depth.

Determination of Local Solar Intensity Input to the Spacecraft

The thermal model segments the spacecraft into thermal nodes. Figure 6 shows the nodes used for this test, along with the definition of aspect angles used in the test series.

The intensity-uniformity of the projected beam was mapped with an X-Y plotting board, as previously described. Figure 7 shows a typical uniformity distribution plot taken with a radiometer; the numbers are millivolt output readings which, when used in conjunction with a

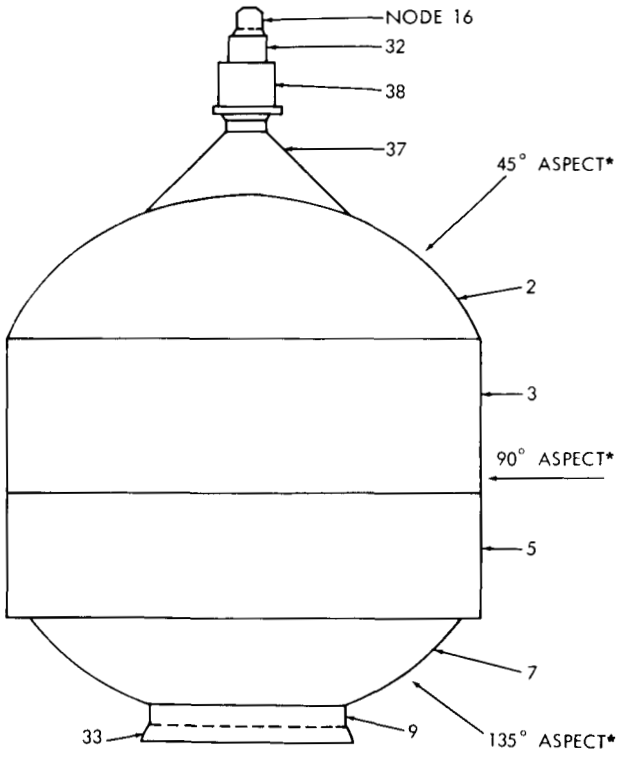

*Angle represents spacecraft-sun aspect, and arrow represents sunlight.

Figure 6–Computer thermal nodes and spacecraft aspect angles.

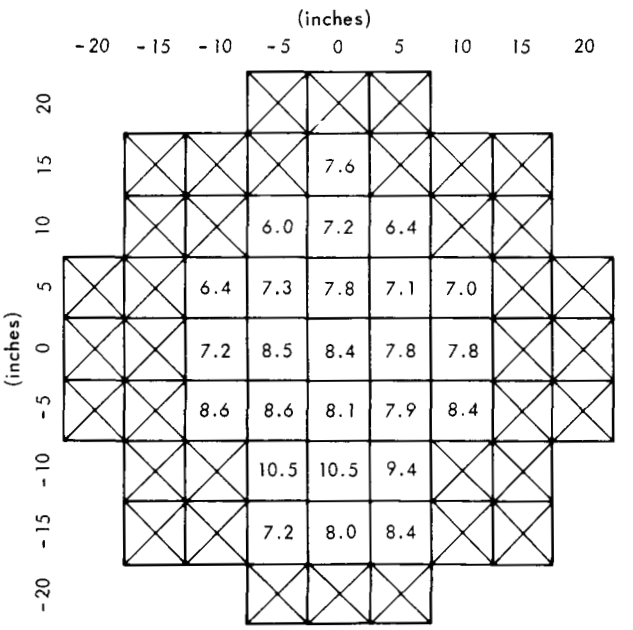

Figure 7–Carbon-arc uniformity distribution survey.

calibration curve, yield relative intensity readings. The uniformity plots were used to determine the local intensity at the individual thermal nodes given in Figure 6. Three planes of intensity perpendicular to the incident beam were plotted: at the spacecraft centerline, 6 inches nearer the beam source, and 12 inches nearer the beam source. This was done to determine the change of intensity with distance from the source, since the beam is diverging at the rate of 7½-degree half-angle. This calibration indicated a change of 6 percent intensity for each position, or a range of 12 percent over the full 12 inches of the beam depth covered. The above information was then used in refining the local intensity values to be used in the thermal analysis.

It should be noted again that, in a reflector-focus arc system, the reflector degrades in performance as it becomes coated with carbon deposit from the open arc. This degradation decreases the total intensity for a given focal length and randomly changes the uniformity pattern as some areas of the reflector receive carbon deposit. Because of this condition, in-test monitoring is necessary to change the arc focal length, compensating for the reflector degradation. Since no adequate real-time in-chamber monitoring device was available, the detector and an X-Y plotting board were used whenever the test schedule called for a simulated shade period in an orbit cycle. These external in-test uniformity plots were then used to indicate the status of the solar flux just prior to the shade period. In addition, they were used to determine what refocusing was necessary to restore the total intensity to the desired 1.01 solar constant. Therefore, a test prediction is made from intensity plots obtained during the test. Table 3 presents the intensity values used for test predictions.

Table 3

Test Chamber Total-Intensity Inputs to the Predict Program*

Spacecraft Node (See Figure 6)	90° Aspect, 100% Sun I_T	90° Aspect, 63-37% Sun I_T	45° Aspect, 100% Sun I_T	135° Aspect, 100% Sun I_T
2	550	597	529	0
3	470	505	492	529
5	468	500	454	484
7	581	496	0	495
9	522	478	0	518
9*	-27	-18	-17	+1.0
16	330	365	728	490
32	330	365	715	504
37	583	729	592	0
38	390	400	689	525

*Notes: 1. Units, Btu/hr-sq ft
2. Total intensity I_T represents available energy to the nodes
3. Node 9* input is conductive energy across the spacecraft rotator interface

SOLAR SIMULATION TEST RESULTS

Figures 8 through 10 present typical thermal profiles that have been included to show the comparison between predicted and test temperatures. From the total data available, the following observations are made:

1. The effect of aspect angle on the mean temperature of the spacecraft, as represented by the battery, was 23 °C.

2. The effect of sunlight-shade exposure time on the mean temperature of the spacecraft was 33 °C. Figure 11, presenting a sample of data from this test, is valuable as an indicator of the interactions of spacecraft structure and components.

3. The temperature excursion of the broadband ozone detector due to sun aspect angle was about 85 °C (69 °C to -17 °C) from test data,

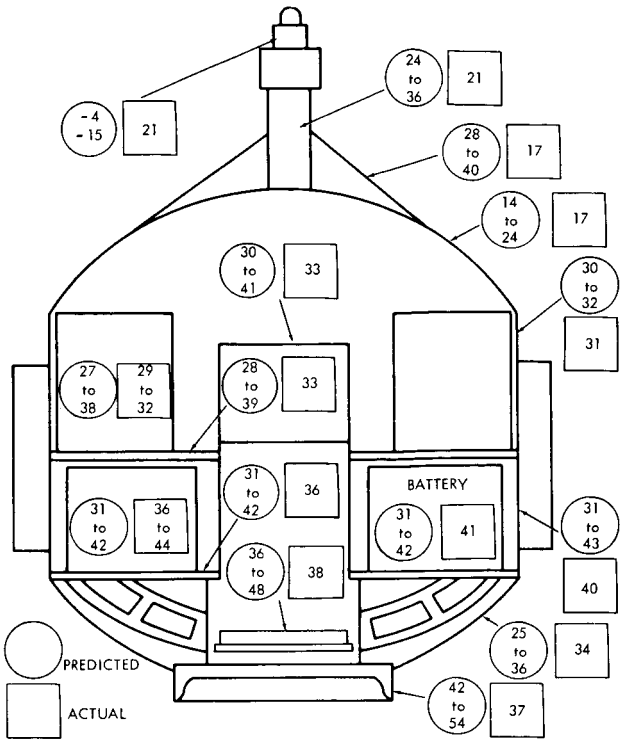

Figure 8—Temperature predictions versus actual test in °C, with 100% sun cycle and 90° aspect angle.

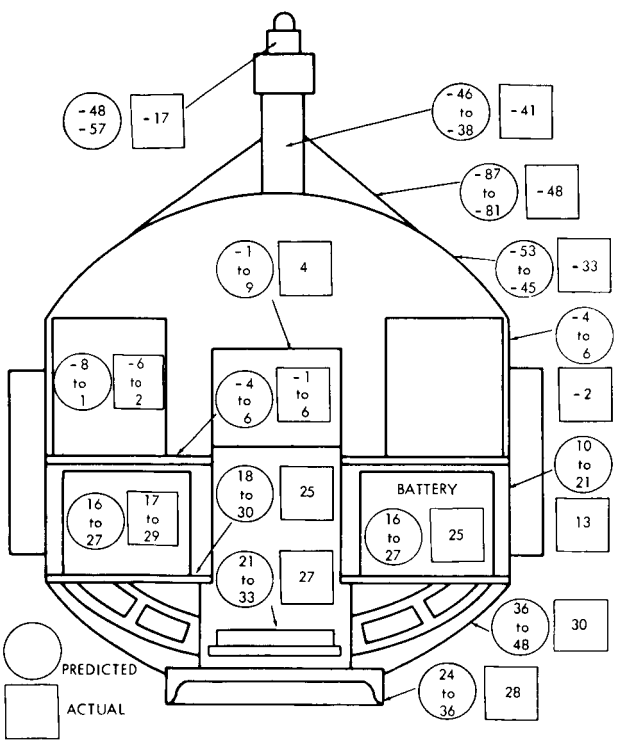

Figure 9—Temperature predictions versus actual test in °C, with 100% sun cycle and 135° aspect angle.

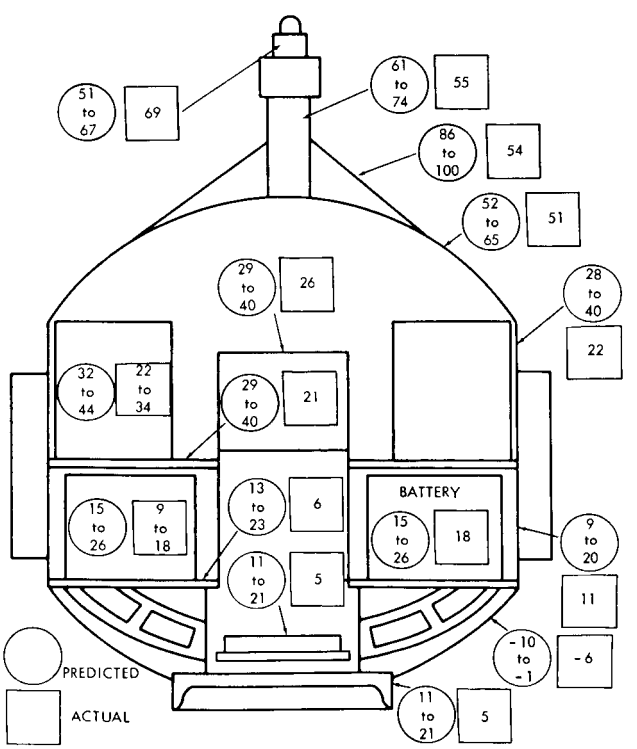

Figure 10*—Temperature predictions versus actual test in °C, with 100% sun cycle and 45° aspect angle.

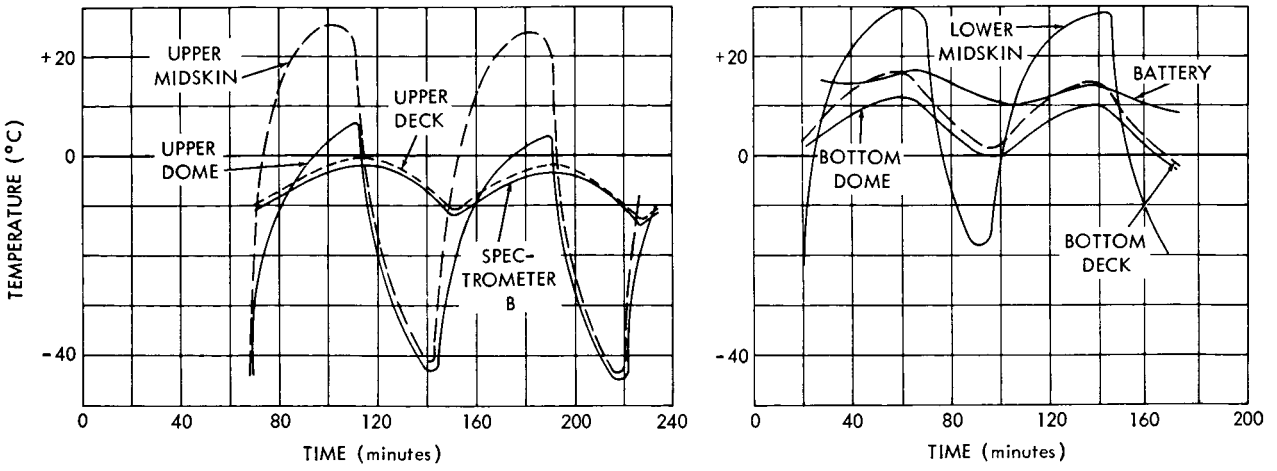

(a) Typical upper deck and skin interaction during cycles

(b) Typical lower deck and skin interaction during cycles

Figure 11—Typical cyclic data.

whereas the predicted excursion was approximately 110°C (59°C to -52° C). The test results indicate that the external portion of the detector does not reach the extreme temperatures that are predicted but more closely follows the temperature of its enclosed base, the support cone, and the top dome.

In addition, it should be noted that two of the experiments required solar energy for activation; thus complete performance was obtained under simulated space conditions.

Also, the occurrence of a coating failure directed attention to a review of the adhesion characteristics under stress and the preparation of surfaces to be painted.

The spacecraft was fully operational throughout the test, and no problems were experienced with components or ground station. One minor exception was an occasional noise interference between the carbon arcs and the spacecraft programmer which controls operating modes of the spacecraft.

CONCLUSIONS

Based on the test results obtained, the following conclusions were reached:

1. The solar simulation test verified the assumptions made for the thermal model, excluding the broadband experiment.

2. The spacecraft should operate satisfactorily under space conditions.

3. The satisfactory performance of the two experiments that were stimulated by simulated solar energy indicates that successful operation should be obtained in space.

4. The carbon arc is a useful solar simulation source although a simulator utilizing optics, rather than reflector focus, would provide better uniformity.

*In Figure 10, test ended prematurely because of data failure, resulting in some low internal temperatures.

5. The nonuniformity of the arc beam intensity can be adequately compensated by the rotating spacecraft and the nodal energy input to the computer program.

(Manuscript received June 12, 1964.)

REFERENCES

1. Hrycak, P., Unger, B. A., and Wittenberg, A. M., "Thermal Testing of the Telstar Satellite," *Proceedings of the Institute of Environmental Sciences, 1963,* p. 377.

2. Hamilton, D. C., and Morgan, W. R., "Radiant-Interchange Configuration Factors," NACA TN-2836, December 1952.

3. Powers, E. I., "Thermal Radiation to a Flat Surface Rotating About an Arbitrary Axis in an Elliptical Earth Orbit: Application to Spin Stabilized Satellites," NASA TN D-2147, January 1964.

NASA-Langley, 1965 G-584N